

Robustness of two-dimensional topological insulator states in bilayer bismuth against strain and electrical field

Li Chen,^{1,2,3,*} Z. F. Wang,² and Feng Liu²¹*Institute of Condensed Matter Physics, Linyi University, Linyi, Shandong 276005, China*²*Department of Materials Science and Engineering, University of Utah, Salt Lake City, Utah 84112, USA*³*State Key Laboratory of Low Dimensional Quantum Physics and Department of Physics, Tsinghua University, Beijing 100084, China*

(Received 23 January 2013; revised manuscript received 17 May 2013; published 18 June 2013)

Using first-principles and Wannier function methods, we systematically calculate the electronic band structure and topological edge states of single bilayer Bi (111) film (BL-Bi) as a function of strain and perpendicular electric field to investigate the effects induced by lattice mismatch and interfacial charge transfer when BL-Bi is epitaxially grown on a substrate. We found that the BL-Bi remains with a finite band gap and a nontrivial band topology for strains up to $\pm 6\%$ and electric fields up to 0.8 eV/\AA . This indicates that the BL-Bi is a robust two-dimensional topological insulator against strain and electrical field on a substrate.

DOI: [10.1103/PhysRevB.87.235420](https://doi.org/10.1103/PhysRevB.87.235420)

PACS number(s): 68.35.Gy, 73.20.At

I. INTRODUCTION

Ultrathin films are essential for many applications in nanoscale science and technology. Thin films are often made by epitaxial growth process supported on a substrate, where interfacial strain due to lattice mismatch and charge transfer due to chemical heterogeneity between the film and substrate are unavoidable. Thus, strain and charge transfer are two important extrinsic factors to alter the intrinsic properties of ultrathin films grown on a substrate. While generally they may be considered as negative factors, we may also work them to our advantage. In fact, strain and interfacial engineering have now become a common strategy to tailor a wide range of thin film properties, from crystalline structure,¹ growth morphology (especially nanoscale assembly),² electronic band structure,³ magnetism,⁴ carrier mobility⁵ to superconductivity.⁶

Recently, a new class of materials of topological insulators (TIs) has been discovered. Among them, two-dimensional (2D) TIs (Refs. 7–16) exist naturally in the thin-film form. So far, theoretical predictions of 2D TI thin films, such as Bi(111) (Refs. 10,11) and Sb(111) (Ref. 12) films have mostly been done for freestanding films assuming a bulk lattice constant, whose topological and electronic properties show a very strong thickness dependence. However, in experiments, these TI films are grown on a substrate. Therefore, an important general question is how interfacial strain and charge transfer will affect the electronic and topological properties of TI films.

Recent experiments have shown that the electronic and topological properties of an ultrathin single BL-Bi depend strongly on the substrate they grow on.^{16–18} It was found when a single BL-Bi is grown on a single quintuple layer (QL) of Bi_2Se_3 or Bi_2Te_3 substrate, an extrinsic helical Dirac band is created by interfacing these two gapped thin films.¹⁷ This extrinsic Dirac state is induced by the Rashba splitting and does not like the surface/edge state in TIs which has a topological origin. Furthermore, when a single BL-Bi is grown on a thick Bi_2Te_3 or Bi_2Se_3 substrate of multiple QLs, distinctively different Dirac bands are formed.¹⁸ On the Bi_2Te_3 substrate, a skewed Dirac cone with nondispersive features is observed indicating many-body interactions that renormalize the linear Dirac bands; while on the Bi_2Se_3 substrate, a normal

Dirac cone is observed indicating absence of many-body interactions.¹⁸

There could be different factors, such as epitaxial strain, structural deformation, molecular orbital hybridization, and interfacial charge transfer, which affect the properties of Bi overlayer. However, experimental and theoretical analyses suggest two effects are most dominating. First, there appears a giant Rashba effect resulting from the internal electrical field induced by interfacial charge transfer when the BL-Bi is grown on either Bi_2Se_3 or Bi_2Te_3 substrate.^{16–18} Second, the in-plane lattice constant is measured to match the substrate exactly with a perfect coherent interface,^{16–18} which means the Bi (111) film is under 3.5% and 9.0% compressive strain on Bi_2Te_3 and Bi_2Se_3 , respectively, so that strain was suggested to play an important role in affecting the degree of many-body interaction of topological band states in addition to internal electrical field effect.¹⁸

Motivated by these recent experiments, we have carried out a systematic study of the electronic properties of BL-Bi focusing on the effects of strain and perpendicular electric field (as a major consequence of interfacial charge transfer), based on first-principles calculations. Our goal is to isolate these two important effects from other possible effects, which might also occur in experiments. We found that the band gap of the BL-Bi can be tuned by both strain and electric field, but without gap closing for strains up to $\pm 6\%$ and electric fields up to 0.8 eV/\AA . Furthermore, our BL-Bi edge-state calculations show that the TI properties of the BL-Bi are unaffected by strain or electric field; there remains always an odd number of edge bands crossing at the Fermi level. These calculation results allow us to conclude that the TI states of BL-Bi is very robust against strain and electric field when grown on a substrate, which can be very useful for future experimental studies as well as advantageous for their potential spintronics applications.

II. METHODS AND PARAMETERS

The BL-Bi (111) has a hexagonal lattice with two atoms per unit cell, as shown in Fig. 1. Its electronic band structures

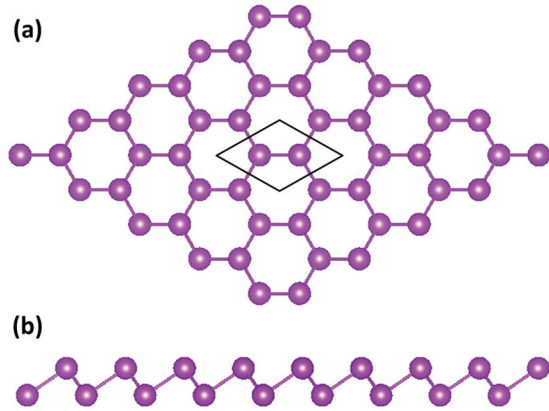


FIG. 1. (Color online) (a) Top view and (b) side view of the Bi-BL(111) atomic structure. The rhombus shows the unit cell.

and electronic properties were calculated as before^{17,18} in the framework of the Perdew–Burke–Ernzerhof (PBE)-type generalized gradient approximation using Vienna *Ab initio* Simulation Package (VASP) package.¹⁹ All calculations are performed with a plane-wave cutoff of 400 eV on a $15 \times 15 \times 1$ Monkhorst-Pack k-point mesh. For structural relaxation, all the atoms are allowed to relax until atomic forces are smaller than 0.01 eV/Å. The optimized lattice constant is $a = 4.35$ Å. The way to handle electric field in VASP is adding an artificial dipole sheet in the middle of the vacuum part in the periodic cell. In our study, the direction of the electric field was chosen to be perpendicular to Bi-BL sheet (along the z direction), and the vacuum layer is ~ 15 Å thick. The edge states of one-dimensional (1D) zigzag BL-Bi nanoribbon (ZBNR) were calculated as before^{20,21} by using

the Wannier90 package.²² The tight-binding Hamiltonian with maximally localized Wannier functions (MLWFs) was fitted to the first-principles calculations. To study the strain and electric field effect, the MLWFs were fitted separately for each electric field and strain configurations in the first-principles calculations. Using this unit cell TB Hamiltonian, we can further construct a supercell Hamiltonian of the ZBNR, containing 40 unit cells.

III. RESULTS AND DISCUSSION

Figure 2(a) shows the band structure of BL-Bi without strain. There is an indirect band gap of 0.56 eV around the Γ point, consistent with previous calculations.^{11,23} The conduction band minimum (CBM) lies exactly at Γ , while the valence band maximum (VBM) lies slightly away from Γ . We also check the orbital components of the CBM and VBM, which come from p orbitals. Figures 2(b) and 2(c) show the typical band structures of BL-Bi under compressive (-3%) and tensile (3%) biaxial strain, respectively. Under compressive strain, the position of VBM shows little change, but the CBM moves towards the M point [Fig. 2(b)]. With the increasing compressive strain, the indirect band gap of BL-Bi increases first (up to about -1%), and then decreases monotonically, as shown in Fig. 2(d). Under tensile strain, the position of VBM shows little change, while the CBM stays at the Γ point [Fig. 2(c)]. With the increasing tensile strain, the indirect band gap of BL-Bi decreases monotonically, as shown in Fig. 2(d).

We then calculate the band structures of BL-Bi in a perpendicular electric field to mimic the interfacial charge transfer effect. As shown in Fig. 3(a), for $E = 0.2$ eV/Å,

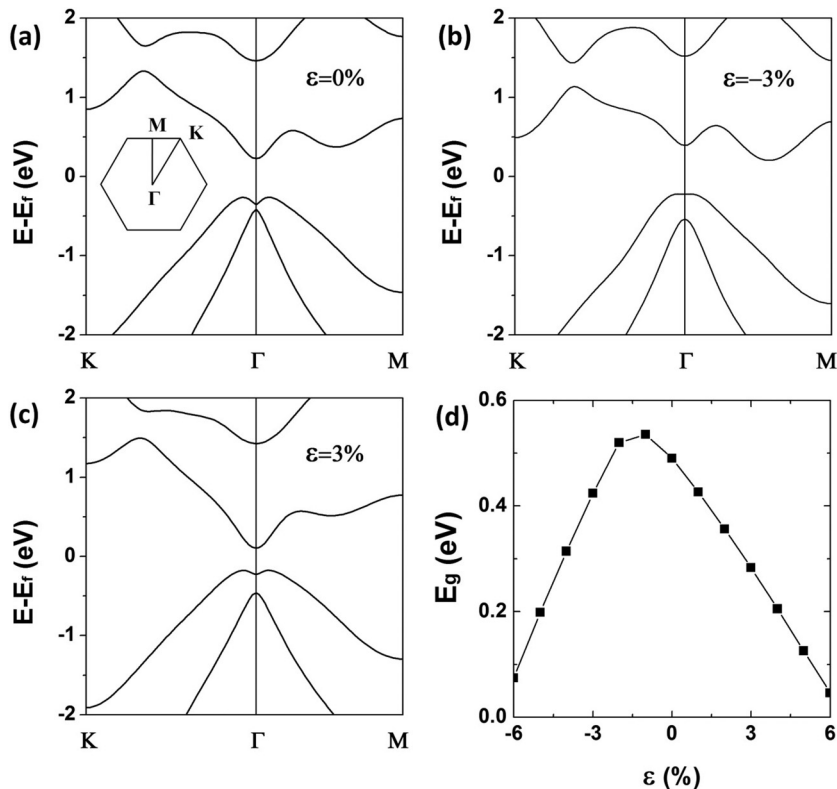


FIG. 2. Band structures of 2D BL-Bi (111) under different strains, (a) 0%, (b) -3% , and (c) 3% . (d) Band gap as a function of strain.

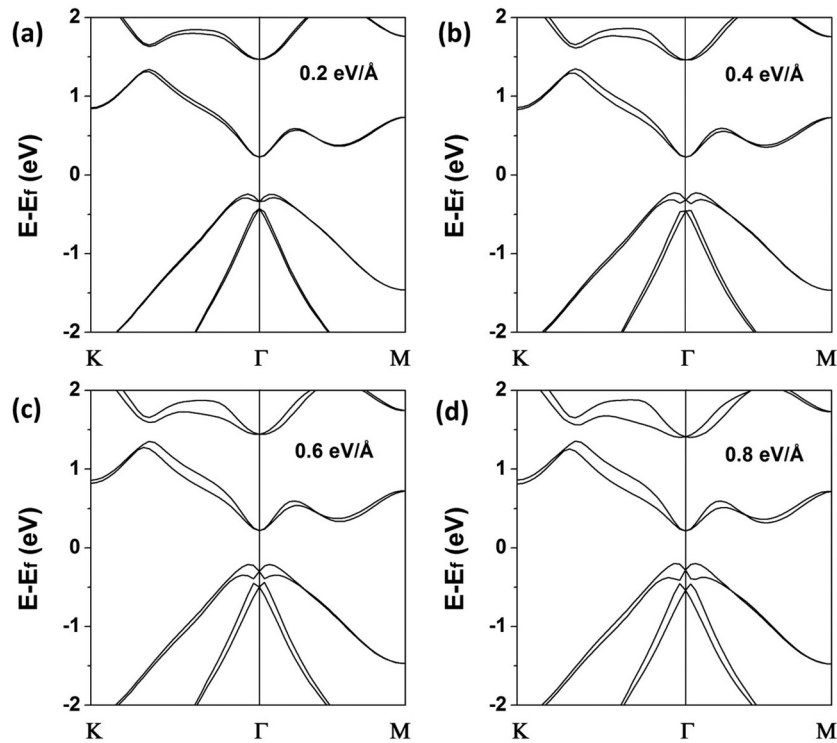


FIG. 3. Band structures of 2D BL-Bi(111) under different electric fields, (a) 0.2, (b) 0.4, (c) 0.6, and (d) 0.8 eV/Å.

the most significant effect of the electric field is to split the band spin-degeneracy. This can be attributed to the Rashba splitting induced by the inversion symmetry breaking in the electric field.^{17,24} With the increasing electric field from 0.2 to 0.8 eV/Å [Figs. 3(a)–3(d)], we found that the band splitting increases continuously. This can be easily understood, as the Rashba splitting is proportional to the intensity of the external

field. One sees that the CBM stays at the Γ point in the electric field, while the VBM moves slightly, so that the band gap decreases slightly with the increasing electric field. Another interesting feature is the VBM splitting results effectively in formation of Dirac bands with almost linear dispersion.¹⁷

The most important finding in band structures is that there is no band gap closing for biaxial strains up to $\pm 6\%$ and

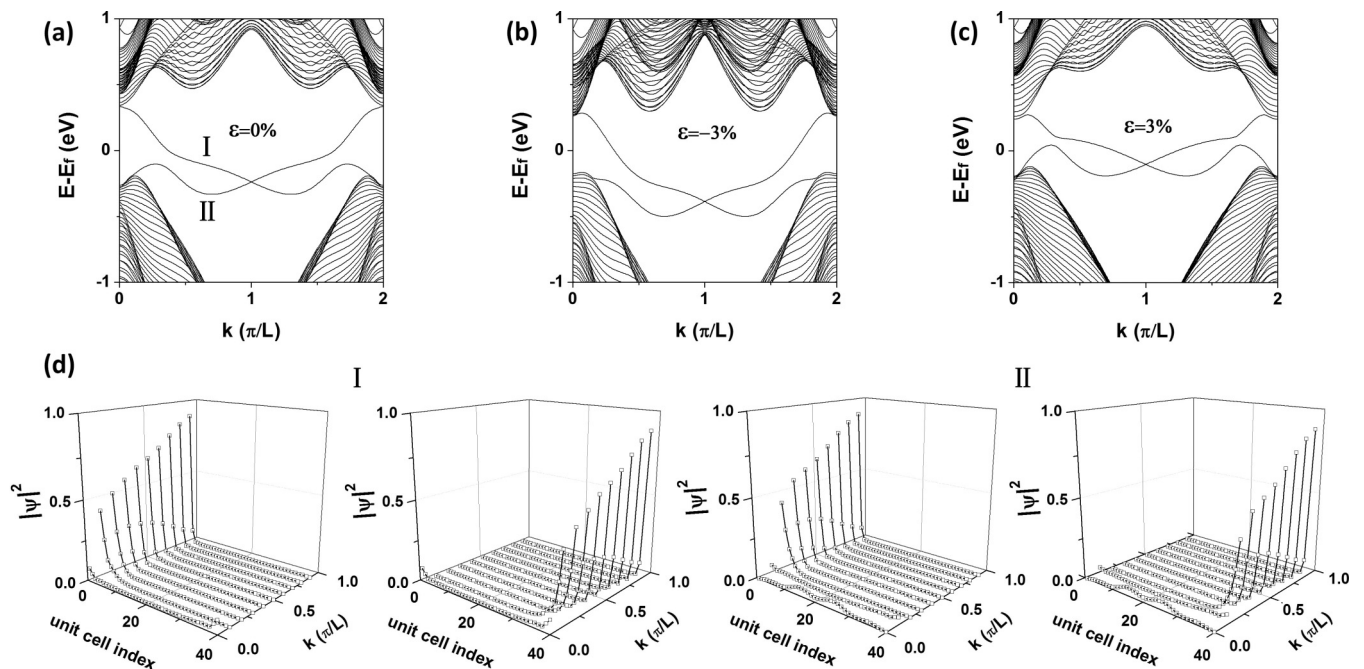


FIG. 4. Band structures of the ZBNR (containing 40 unit cells) under different strains, (a) 0%, (b) -3% , and (c) 3% . (d) Spatial distribution of the edge-state wave functions in (a). I and II label the different edge states, which are energy degenerate for different edges. The wave function is plotted as a function of the unit-cell position within the supercell and k point. Here, $|\psi|^2$ is the total wave function within each unit cell.

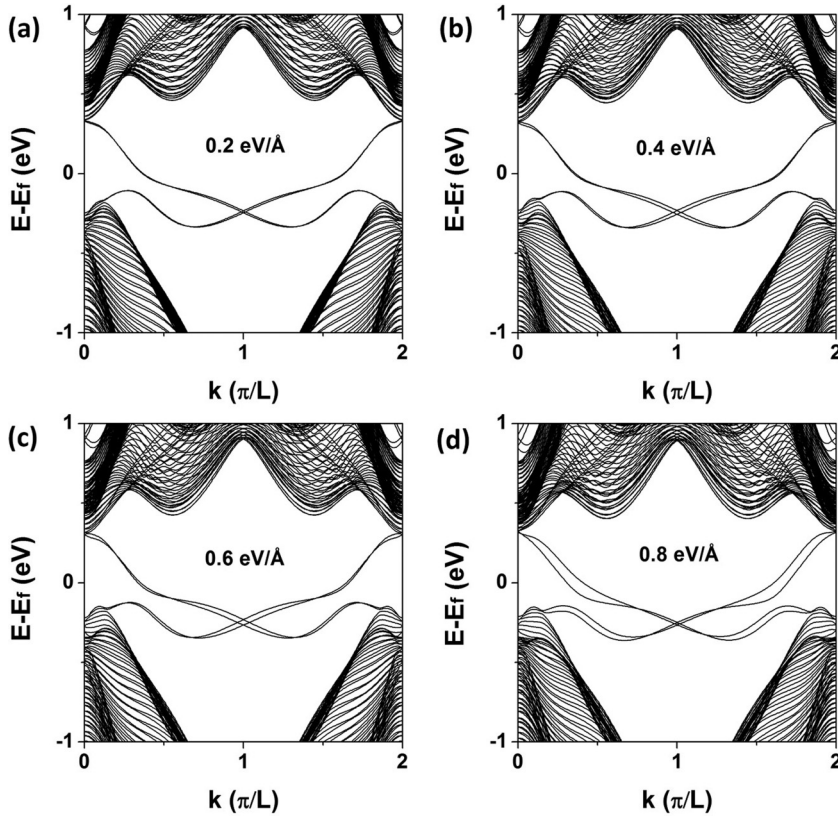


FIG. 5. Band structures of the ZBNR (containing 40 unit cells) under different electric fields, (a) 0.2, (b) 0.4, (c) 0.6, and (d) 0.8 eV/Å.

perpendicular electric fields up to 0.8 eV/Å. This indicates that the electronic properties of Bi-BL are likely to be very robust against strain and/or interfacial charge transfer. To further confirm this point, we have calculated the 1D edge states of the ZBNR, which gives a direct manifestation of the electronic properties.

Figure 4(a) shows the edge states of ZBNR without strain, exhibiting clearly a 1D Dirac edge state (the Dirac point is at the boundary of the Brillouin zone, $k = \pi/L$) inside the “bulk” band gap. The 1D Dirac edge state is spin degenerated, i.e. the spatially separated edge states at the two edges of the ZBNR are energy degenerated, but with different spin orientations. For each edge state, there is only one band-crossing point at the Fermi level in half of the Brillouin. Tuning the Fermi level within the band gap region, the property of an odd number of band-crossing points remains intact. Therefore, the strain-free BL-Bi (111) is an intrinsic 2D TI.^{10,11} The spatial distributions of these edge states are shown in Fig. 4(d). At the Brillouin zone boundary, the edge-state wave function is localized at the edge. However, as the k decreases from the zone boundary to the center, the edge-state wave function gradually becomes delocalized. These results are consistent with previous theoretical calculations.^{14,24} For the strained ZBNR, their corresponding band structures are shown in Figs. 4(b) and 4(c) under -3% and 3% strain, respectively. Except for the relative shape change, the properties of edge states are essentially the same to the strain-free case, particularly there is always a Dirac edge band within the band gap, which has an odd number of band-crossing points in half of the Brillouin. Therefore, the BL-Bi remains an intrinsic 2D TI under these strain conditions. The different shape of the edge states in

Fig. 4 can be attributed to the atomic structure change under the strain, but it does not change the band topology. Under the strain (-3% and 3%), the edge-state distributions show little change, which are similar to the result without strain [Fig. 4(d)].

In addition, we have also checked the electronic structures of BL-Bi under larger strains up to -10% and 10% . For compressive strain beyond 7% , the BL-Bi will close its band gap becoming a metal; for tensile strain beyond 7% , the band gap of BL-Bi will increase with the increasing tensile strain after decreasing initially. One-dimensional edge state calculations further show that the BL-Bi remains a 2D TI up to 10% tensile strain without topological phase transition.

Lastly, the band structures of ZBNR under electric field are calculated, as shown in Fig. 5. The electric field breaks the inversion symmetry of the whole ribbon and results in a different electrostatic potential at the two edges, as one edge has the “up” atom position while the other edge has the “down” atom position. Consequently, the energy-degenerated edge states (with opposite spins at the two edges) are slightly split under the electric field, and we see two Dirac points at the boundary of the Brillouin zone in the electric field. The splitting of the spin degeneracy and thence the separation between the two Dirac points changes slightly with the strength of electric field [Figs. 5(a)–5(d)]. However, the nontrivial topological properties of the edge states are not changed by the electric field; each Dirac band still has an odd number of band-crossing points with the Fermi level within the band gap region in half of the Brillouin zone. So, the BL-Bi remains a 2D TI under the electric field up to 0.8 eV/Å.

IV. CONCLUSIONS

In conclusion, we have carried out a systematic study of electronic properties of single BL-Bi under strain and electric field. Our calculations show that, although the band gap of BL-Bi may overall decrease with either compressive or tensile strain, a finite gap can survive for strains up to $\pm 6\%$, and also the nontrivial topological edge states preserve within the gap. The main effect of electric field is found to be splitting the spin degeneracy of bands but with little influence on band topology that remains nontrivial for the electric field up to 0.8 eV/\AA . These results unequivocally demonstrate that the electronic properties of the BL-Bi are very robust against the external influences of strain and electrical field, easing its growth and application on a foreign substrate.

ACKNOWLEDGMENTS

L.C. thanks Dr. Hua Jiang for helpful discussions. L.C. thanks financial support from the National Natural Science Foundation of China (Grant Nos. 10974076, 11274151, 11147007, 11204120), Open Research Fund Program of the State Key Laboratory of Low-Dimensional Quantum Physics (Grant No. 20120924) and Key Disciplines of Condensed Matter Physics of Linyi University. ZFW and FL thank support from US DOE-BES (Grant No. DE-FG02-04ER46148). ZFW also acknowledges support from ARL (Cooperative Agreement No. W911NF-12-2-0023). We also thank the CHPC at University of Utah and Linyi University for providing the computing resources.

*Corresponding author: lchen.lyu@gmail.com

¹D. Wu, M. G. Lagally, and F. Liu, *Phys. Rev. Lett.* **107**, 236101 (2011).

²H. Hu, H. J. Gao, and F. Liu, *Phys. Rev. Lett.* **101**, 216102 (2008).

³Z. Liu, J. Wu, W. Duan, M.G. Lagally, and F. Liu, *Phys. Rev. Lett.* **105**, 016802 (2010).

⁴D. Sander, S. Ouazi, A. Enders, Th. Gutjahr-Loser, V. S. Stepanyuk, D. I. Bazhanov, and J. Kirschner, *J. Phys.: Condens. Matter* **14**, 4165 (2002).

⁵D. Yu, Y. Zhang, and F. Liu, *Phys. Rev. B* **78**, 245204 (2008).

⁶D. C. van der Laan and J. W. Ekin, *Appl. Phys. Lett.* **90**, 052506 (2007).

⁷C. L. Kane and E. J. Mele, *Phys. Rev. Lett.* **95**, 226801 (2005).

⁸B. A. Bernevig, T. L. Hughes, and S. C. Zhang, *Science* **314**, 1757 (2006).

⁹M. König, S. Wiedmann, C. Brüne, A. Roth, H. Buhmann, L.W. Molenkamp, X. L. Qi, and S. C. Zhang, *Science* **318**, 766 (2007).

¹⁰S. Murakami, *Phys. Rev. Lett.* **97**, 236805 (2006).

¹¹Z. Liu, C. X. Liu, Y. S. Wu, W. H. Duan, F. Liu, and J. Wu, *Phys. Rev. Lett.* **107**, 136805 (2011).

¹²P. F. Zhang, Z. Liu, W. Duan, F. Liu, and J. Wu, *Phys. Rev. B* **85**, 201410(R) (2012).

¹³T. Hirahara, G. Bihlmayer, Y. Sakamoto, M. Yamada, H. Miyazaki, S. I. Kimura, S. Blügel, and S. Hasegawa, *Phys. Rev. Lett.* **107**, 166801 (2011).

¹⁴F. Yang, L. Miao, Z. F. Wang, M. Y. Yao, F. Zhu, Y. R. Song, M. X. Wang, J. P. Xu, A. V. Fedorov, Z. Sun, G. B. Zhang, C. Liu, F. Liu, D. Qian, C. L. Gao, and J. F. Jia, *Phys. Rev. Lett.* **109**, 016801 (2012).

¹⁵H. Zhang, F. Freimuth, G. Bihlmayer, S. Blügel, and Y. Mokrousov, *Phys. Rev. B* **86**, 035104 (2012).

¹⁶T. Hirahara, N. Fukui, T. Shirasawa, M. Yamada, M. Aitani, H. Miyazaki, M. Matsunami, S. Kimura, T. Takahashi, S. Hasegawa, and K. Kobayashi, *Phys. Rev. Lett.* **109**, 227401 (2012).

¹⁷Z. F. Wang, M. Y. Yao, W. Ming, L. Miao, F. Zhu, C. Liu, C. L. Gao, D. Qian, J. F. Jia, and F. Liu, *Nat. Commun.* **4**, 1384 (2013).

¹⁸L. Miao, Z. F. Wang, W. Ming, M. Y. Yao, M. X. Wang, F. Yang, F. Zhu, A. V. Fedorov, Z. Sun, C. L. Gao, C. Liu, Q. K. Xue, C. X. Liu, F. Liu, D. Qian, and J. F. Jia, *Proc. Natl. Acad. Sci. USA* **110**, 2758 (2013).

¹⁹G. Kresse and J. Hafner, *Phys. Rev. B* **47**, 558 (1993).

²⁰M. Wada, S. Murakami, F. Freimuth, and G. Bihlmayer, *Phys. Rev. B* **83**, 121310 (2011).

²¹Z. F. Wang, Z. Liu, and F. Liu, *Nat. Commun.* **4**, 1471 (2013).

²²A. A. Mostofi, J. R. Yates, Y. S. Lee, I. Souza, D. Vanderbilt, and N. Marzari, *Comput. Phys. Commun.* **178**, 685 (2008).

²³Yu. M. Koroteev, G. Bihlmayer, E. V. Chulkov, and S. Blügel, *Phys. Rev. B* **77**, 045428 (2008).

²⁴H. Kotaka, F. Ishii, M. Saito, T. Nagao, and Shin Yaginuma, *Jpn. J. Appl. Phys.* **51**, 025201 (2012).